# Phosphorylation-Induced Structural Change in Phospholamban and Its Mutants, Detected by Intrinsic Fluorescence†

Ming Li,‡ Razvan L. Cornea,‡ Joseph M. Autry,§ Larry R. Jones,§ and David D. Thomas*,‡

*Department of Biochemistry, University of Minnesota Medical School, Minneapolis, Minnesota 55455, and Krannert Institute of Cardiology, Indiana University, Indianapolis, Indiana 46202*

*Received January 14, 1998; Revised Manuscript Received March 27, 1998*

ABSTRACT: We have used intrinsic fluorescence to test the hypothesis that phosphorylation induces a conformational change in phospholamban (PLB), a regulatory protein in cardiac sarcoplasmic reticulum (SR). Phosphorylation of PLB, which relieves inhibition of the cardiac Ca-ATPase, has been shown to decrease the mobility of PLB in sodium dodecyl sulfate−polyacrylamide gel electrophoresis (SDS−PAGE). In the present study, we found that this mobility shift depends on the acrylamide concentration in the gel, suggesting that phosphorylation increases the effective Stokes radius. To further characterize this structural change, we performed spectroscopic experiments under the conditions of SDS−PAGE. CD indicated that phosphorylation at Ser-16 does not change PLB's secondary structure significantly. However, the fluorescence of Tyr-6 in the cytoplasmic domain of PLB changed significantly upon PLB phosphorylation: phosphorylation increased the fluorescence quantum yield and decreased the quenching efficiency by acrylamide, suggesting a local structural change that decreases the solvent accessibility of Tyr-6. A point mutation (L37A) in the transmembrane domain, which disrupts PLB pentamers and produces monomers in SDS−PAGE and in lipid bilayers, showed similar phosphorylation effects on fluorescence, indicating that subunit interactions within PLB are not crucial for the observed conformational change in SDS. When PLB was reconstituted into dioleoylphosphatidylcholine (DOPC) lipid bilayers, similar phosphorylation effects in fluorescence were observed, suggesting that PLB behaves similarly in response to phosphorylation in both detergent and lipid environments. We conclude that phosphorylation induces a structural change within the PLB protomer that decreases the solvent accessibility of Tyr-6. The similarity of this structural change in monomers and pentamers is consistent with models in which the PLB monomer is sufficient for the phosphorylation-dependent regulation of the Ca-ATPase.

In cardiac sarcoplasmic reticulum (SR),[1] the activity of the calcium pump (Ca-ATPase) is regulated by phospholamban (PLB), a 52 amino acid integral membrane protein (*1*, *2*). PLB inhibits and aggregates the Ca-pump under resting conditions in the heart (*3*, *4*). Upon $\beta$-adrenergic stimulation, PLB is phosphorylated at both Ser-16 (by cAMP-dependent protein kinase) and Thr-17 (by CAM kinase) (*5*), which relieves the inhibition (*6*, *7*) and causes Ca-pump aggregates to dissociate (*4*).

The molecular mechanism of this regulation is unclear. Since phosphorylation reduces the charge on the cytosolic domain of PLB (from +3 to +1), this probably decreases electrostatic interactions with the negatively charged Ca-pump and facilitates dissociation of PLB from it (*8*, *4*). However, structural changes within PLB upon phosphorylation may also be required for the mechanism of regulation (*9*, *10*).

Sodium dodecyl sulfate−polyacrylamide gel electrophoresis (SDS−PAGE) provided the first evidence for a structural change of PLB upon phosphorylation: On SDS−PAGE, PLB is predominantly pentameric, and the mobility of the pentamer decreases upon phosphorylation (*11*, *12*). This mobility shift could be due simply to the change in electrostatic charge, possibly affecting SDS binding, or to a change in protein conformation, or both. A phosphorylation-induced mobility shift on SDS−PAGE has been observed in several other proteins, but the mechanism is not clear (*13*, *14*). One of the goals of this research is to assess the mechanism for this phosphorylation-induced mobility shift.

Several spectroscopic techniques have been used to investigate structural changes of PLB upon phosphorylation (*15*, *16*, *9*, *10*, *17*). There remains controversy whether a significant conformational change occurs upon PLB phosphorylation, and whether the change involves secondary or tertiary structural features. Some spectroscopic studies report changes in the secondary structure of PLB upon phospho-

† This work was supported by Grants to D.D.T. from the National Institutes of Health (GM27906) and the Minnesota Supercomputer Institute. L.R.J. was suported by grants (HL06308 and HL49428) from the National Institutes of Health. J.M.A. was supported by a Predoctoral Fellowship from the American Heart Association, Indiana Affiliate.

* To whom correspondence should be addressed.

‡ University of Minnesota Medical School.

§ Indiana University.

[1] Abbreviations: CD, circular dichroism; PLB, phospholamban; SR, sarcoplasmic reticulum; SDS, sodium dodecyl sulfate; SDS−PAGE, sodium dodecyl sulfate−polyacrylamide gel electrophoresis; DOPC, dioleoylphosphatidylcholine; cAMP, cyclic adenosine monophosphate; ATP, adenosine triphosphate; PKA, cAMP-dependent protein kinase; CSU, catalytic subunit of PKA; CAM, calmodulin; OG, octyl $\beta$-D-glucopyranoside; SEM, standard error of the mean; EPR, electron paramagnetic resonance.

S0006-2960(98)00105-6 CCC: $15.00 
Published on Web 05/06/1998

rylation (*9*, *10*, *18*), while others do not (*15*, *17*). A problem contributing to the controversy is that most of the techniques employed (e.g., circular dichroism, nuclear magnetic resonance, infrared spectroscopy) are not equally applicable in solution and in lipid bilayers. This is not a problem for fluorescence, which has not been applied previously to PLB. PLB has a single intrinsic fluorophore, Tyr-6, which constitutes a convenient spectroscopic sensor for local conformation within the N-terminal cytoplasmic domain.

The goals of the present study were to determine whether the phosphorylation-induced shift observed on SDS−PAGE corresponds to a fluorescence-detectable structural change within PLB, whether this change depends on oligomeric interactions of PLB, and whether this change also occurs when PLB is in its native state in lipid bilayers. We used fluorescence and circular dichroism (CD) spectroscopy to study wild-type PLB (WT-PLB), a mutant that is monomeric on SDS−PAGE (L37A-PLB, Leu-37 replaced by Ala), and another mutant in which Tyr-6 is mutated to Trp-6 (Y6W-PLB). The studies were done both on PLB in solution in the buffer used for SDS−PAGE and on PLB reconstituted into a lipid bilayer.

## MATERIALS AND METHODS

*Reagents and Solutions.* Catalytic subunit (CSU) of PKA purified from porcine heart, adenosine triphosphate (ATP), octyl $\beta$-D-glucopyranoside (OG), SDS, and acrylamide were purchased from Sigma Chemical Co. (St. Louis, MO). Dioleoylphosphatidylcholine (DOPC) was obtained from Avanti Polar Lipids (Alabaster, AL). The reagents for SDS−PAGE were purchased from Bio-Rad Laboratories (Richmond, CA). The phosphatase inhibitor calyculin A was obtained from LC Laboratories (San Diego, CA). Endoproteinase Lys-C (sequencing grade) was from Boehringer Mannheim (Indianapolis, IN). SDS−PAGE running buffer contained 0.2 M Tris, 0.6 M glycine, and 0.1% SDS, pH 8.3. DOPC buffer contained 20 mM MOPS, 5 mM $MgCl_2$, pH 7.0. Most spectroscopic measurements were performed in one of these two buffers, at a temperature of 25 ± 1 °C.

*Preparation of PLB.* Recombinant wild-type (WT-PLB) and the mutant L37A-PLB were expressed and purified using Sf21 insect cells infected by recombinant baculovirus, as previously described (*19*, *20*). The purified proteins were stored at −70 °C, at a protein concentration of 2.27 mg/mL for WT-PLB and 1.09 mg/mL for L37A-PLB, in a buffer containing 18 mM glycine, 88 mM MOPS, 5 mM DTT, and 0.92% OG, pH 7.2. Protein concentrations were determined by the amido black assay (*21*). Site-direct mutagenesis for Y6W was conducted as described (*20*). Y6W-PLB was expressed and purified from Sf21 cells by the same method and stored at a protein concentration of 2.17 mg/mL. The N-terminus of Y6W-PLB was blocked like that of WT-PLB and L37A-PLB. After treatment of Y6W-PLB with endoproteinase Lys-C to cleave the protein at lysine residue 3, the presence of tryptophan residue 6 was confirmed by direct sequence analysis. Protein concentrations were determined by the amido black assay (*21*), with a precision of ±4%.

*Reconstitution of PLB into Lipid Bilayers.* Lipid bilayers containing PLB were prepared essentially as described previously (*22*): a solution containing 160 $\mu$M PLB in 0.9% OG, 100 mM KCl, 20 mM MOPS, pH 7.0, was added to a dried film of DOPC, usually at a ratio of 100 mol of lipid/mol of PLB. The mixture was incubated at room temperature for 1 h with frequent vortexing. Then 300 $\mu$L of 20 mM MOPS, 100 mM KCl, pH 7.0 (reconstitution buffer), was added to the mixture, and the sample was subjected to 15 min incubation with vortexing and 5 min sonication in a water bath. The sample was then diluted with another 5.7 mL of reconstitution buffer and centrifuged in a Beckman TL-100 centrifuge at 100 000 rpm for 1 h. The pellet was resuspended in 90 $\mu$L of DOPC buffer.

*Phosphorylation of PLB.* For phosphorylation in detergent, 40 $\mu$g of purified WT-PLB or L37A-PLB was incubated at 30 °C, for 12 h, in 92 $\mu$L of a buffer containing 20 mM MOPS, 5 mM $MgCl_2$, 50 nM calyculin A, and 0.9% OG, pH 7.0 (phosphorylation buffer). The phosphorylated sample contained 130 IU/mL CSU, while CSU was omitted from the control (unphosphorylated) sample. The phosphorylation reaction was initiated by adding ATP to a final concentration of 0.6 mM. The reaction was stopped with concentrated SDS−PAGE running buffer. To phosphorylate lipid-reconstituted PLB, we used the same procedure, but in order to ensure the access of CSU and ATP to occluded PLB, we included a freeze−thaw step after the addition of ATP. These samples were then subjected to electrophoresis, fluorescence, and CD measurements. PLB phosphorylation was characterized by both SDS−PAGE (mobility shift) and $^{32}$P-autoradiography (using [$\gamma$-$^{32}$P]ATP). Phosphorylation of L37A-PLB was characterized only by $^{32}$P-autoradiography. The gels were dried and subjected to autoradiography in order to visualize the $^{32}$P-labeled protein. For quantitation, the phosphorylated protein band was excised and subjected to scintillation counting using [$^{32}$P]ATP as a standard. PLB concentration was determined by the amido black assay (*21*). We measured 0.80 ± 0.06 (SEM, $n = 4$) mol of phosphate incorporated per mole of protomer for WT-PLB in solution. Similar phosphorylation levels were observed for L37A-PLB in solution and for the lipid-reconstituted samples.

*Endoproteinase Lys-C Treatment.* WT-PLB was reacted with endoproteinase Lys-C at a ratio of PLB/Lys-C = 60 (w/w) in a buffer of 0.1 M $NaHCO_3$, pH 9, and 0.1% SDS, at 30 °C overnight. The molar percent of PLB being cleaved was measured as 86% by TNBS (2,4,6-trinitrobenzenesulfonic acid) assay. A final concentration of 1 mM TNBS was added to the reaction mixture to incubate at room temperature for 30 min, and the absorbance at 420 nm was then measured to determine the amount of free N-terminus being released by endoproteinase Lys-C. A sample that contained an equal amount of WT-PLB without endoproteinase Lys-C treatment was used as control.

*Ferguson Plot.* This is a method for analysis of SDS−PAGE data that can distinguish a change in the size or shape of a protein from a change in the charge (*23*, *24*). To construct a Ferguson plot, SDS−PAGE is run with various acrylamide concentrations, and then log ($R_m$) is plotted *vs* the acrylamide concentration, where $R_m$ is the electrophoretic mobility, calculated as the distance from the top of the gel to the protein band, divided by the distance from the top of the gel to the dye front. The Ferguson plot is usually linear with negative slope; the slope and intercept depend on the electrical charge of the protein and on the effective hydrated radius of the protein−detergent complex (Stokes radius). A series of model system studies have shown that two proteins

differing only in Stokes radius give different slopes with a common *y*-axis intercept, while two proteins differing only in charge give identical slopes with different *y*-axis intercepts (*24*). In the present study, SDS−PAGE was performed using a method similar to that of Porzio and Pearson (*25*), as described previously (*26*), except that we used a mini-gel system (8 cm × 10 cm). The acrylamide concentration in the gels was varied from 8 to 15%.

*Fluorescence.* Fluorescence measurements were performed in 3 mm × 3 mm quartz cuvettes. For measurements in solution, the protein concentration was 60 $\mu$M and the buffer was usually the same as the SDS−PAGE running buffer. For measurements of PLB in DOPC, the protein concentration was 160 $\mu$M and we used DOPC buffer. The fluorescence emission spectrum of each sample was recorded using a SPEX-Fluorolog II spectrofluorometer (Edison, NJ). For tyrosine fluorescence, the spectra were recorded with excitation at 275 nm, and the excitation wavelengths were 290 nm for tryptophan fluorescence. Both excitation and emission bandwidths were set at 7 nm, so light scattering had no significant effect on the emission, as verified by scanning the emission near the excitation wavelengths. Each spectrum was the average of 20 scans, with a step size of 1 nm and an integration time of 1 s/step. Each fluorescence spectrum was corrected by subtracting the corresponding control spectrum of the buffer without PLB, which has intensities of less than 1/20 of that of the sample spectrum. The emission maximum was determined first by calculating the second derivative of the emission spectrum to find the peak positions, and then using these as the starting parameters to fit the spectra to multiple Lorentzian distributions to confirm the results. Total fluorescence was measured by integrating the spectra.

*Fluorescence Quenching by Acrylamide.* The fluorescence intensities of PLB and its mutants were measured as a function of the concentration of acrylamide, added from a stock solution of 6 M in the appropriate buffer. Collisional quenching of fluorescence is described by the Stern−Volmer equation:

$$F_0/F = 1 + k_q\tau_0[Q] = 1 + k_q c F_0[Q] \quad (1)$$

where $F$ is the fluorescence intensity in the presence of quencher and $F_0$ is the fluorescence intensity in the absence of quencher. $k_q$ is the bimolecular quenching constant, and is dependent on the accessibility of fluorophore to the solvent. $\tau_0$ is the lifetime of the fluorophore in the absence of quencher. [Q] is the concentration of quencher and $c = \tau_0/F_0$, and is a constant. In order to account for the lifetime difference between phosphorylated and unphosphorylated samples, quenching data were presented as a plot of $F_0/F$ versus [Q′]:

$$F_0/F = 1 + k_q c F_0(-P)[Q'] \quad (2)$$

$$[Q'] = [Q]F_0/F_0(-P) \quad (3)$$

$F_0(-P)$ is the fluorescence intensity of the unphosphorylated protein in the absence of quencher. The slope of the plot is $k_q cF_0(-P)$, and any change in the slope reflects a proportional change in $k_q$, which increases with the solvent accessibility of the fluorophore. Each plot was fitted to a straight line using the first five data points, in order to obtain a value for the initial slope.

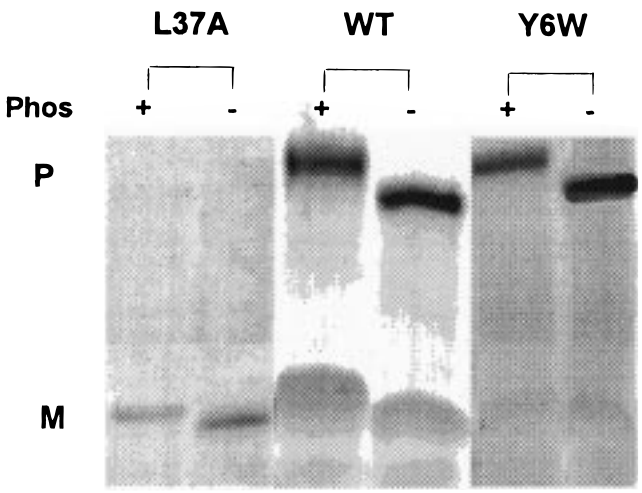


FIGURE 1: Effect of phosphorylation on SDS−PAGE of recombinant WT-PLB, L37A-PLB, and Y6W-PLB. Bands show Coomassie blue stain of unphosphorylated (−) and phosphorylated (+) proteins. The gel contained 16.5% acrylamide with the Tris−Tricine buffer system. Each lane contained 3 $\mu$g of protein. P and M are the pentameric and monomeric forms of PLB.

*Circular Dichroism.* Protein samples that were used for fluorescence measurements in SDS solution were also used for CD measurements. CD spectra were recorded on a JASCO J-710 spectropolarimeter (Tokyo, Japan) over the wavelength range of 190−260 nm in a 0.1 mm path-length cell. Buffer blanks were subtracted. The scan speed was 20 nm/min. Each spectrum was the average of four scans. The α-helix content was determined by a computer program, Selcon, from the Jasco manufacturer (Tokyo, Japan) that uses a self-consistent method and relies on a database of known protein structures (*27*).

## RESULTS

*Electrophoretic Analysis of PLB Phosphorylation.* In SDS−PAGE, WT-PLB displayed a distribution between pentamer (Figure 1, P) and monomer (Figure 1, M), and phosphorylation at Ser-16 by protein kinase A decreased the mobility of both species, as shown previously (*11*). Phosphorylation decreased the pentamer mobility by 16 ± 2% (SEM, $n = 6$), corresponding to an increase in the apparent molecular mass from 25 to 27 kDa. In order to determine the importance of oligomeric interactions for the phosphorylation-induced gel shift, we studied the PLB mutant L37A, in which Leu-37 has been mutated to Ala. Figure 1 shows that this protein is monomeric on SDS−PAGE (*20*), and that it undergoes a significant mobility decrease (7% ± 3%) upon phosphorylation (*22*), indicating that oligomeric interactions are not required for this gel shift. Another mutant of PLB, Y6W, in which Tyr-6 was mutated to Trp, was also studied. Figure 1 shows that Y6W-PLB has the same mobility as that of WT-PLB, and that phosphorylation causes a similar gel shift in Y6W-PLB.

The phosphorylation-induced gel shift is not due to a change in the oligomeric state of PLB (*12*, *28*), so it is probably due to a change in either electrostatic charge or protein conformation. To distinguish between these two possibilities, we carried out SDS−PAGE as a function of acrylamide concentration (Ferguson plot, Figure 2). For

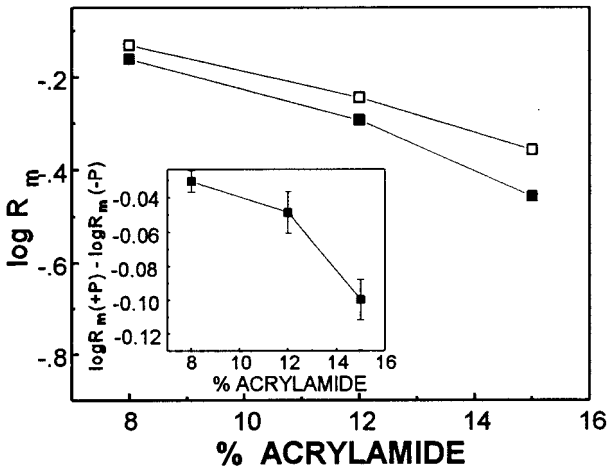


FIGURE 2: Dependence of electrophoretic mobility ($R_m$) of the PLB pentamer band (Figure 1, P) on acrylamide concentration (%, w/v) in SDS−PAGE (Ferguson plot). (□) Unphosphorylated (−P). (■) Phosphorylated (+P). Inset: difference plot between the phosphorylated and unphosphorylated forms of PLB. Slope: log $R_m$(+P) − log $R_m$(−P). Each error bar shows the range of three measurements.

Table 1: Effects of Phosphorylation on Tyr-6 and Trp-6 Fluorescence of WT, L37A, and Y6W-PLB[a]

| % increase upon phosphorylation | WT | L37A | Y6W |
|---|---|---|---|
| in SDS | 23 ± 8[b] | 21 ± 5 | 5 ± 1 |
| in OG | 23 ± 3 | 21 ± 3 | 45 ± 4 |
| in DOPC | 23 ± 2 | 20 ± 6 | 42 ± 5 |

[a] Fluorescence was measured by integrating the spectra in Figure 3. [b] Mean ± SEM; $n = 6$ for WT-PLB, $n = 4$ for the mutants L37A and Y6W.

unphosphorylated PLB, the logarithm of mobility decreased linearly with the acrylamide concentration (Figure 2, open squares), as observed previously (*29*). Phosphorylation decreased the mobility, with a greater effect as the acrylamide concentration increased (Figure 2, closed squares), resulting in a significantly steeper slope in the Ferguson plot. If the mobility decrease were caused only by a change in the charge on PLB, it would be independent of the acrylamide concentration, and the difference plot (Figure 2, inset) would have zero slope (*23*, *24*). The negative slope of the difference plot indicates that phosphorylation causes a structural change that increases the effective Stokes radius of PLB.

*Intrinsic Fluorescence of PLB in Detergents and Lipid Bilayers*. In order to determine the relationship between the structural changes suggested by SDS gels and the structural changes that might occur under more physiological conditions in a lipid membrane in the absence of SDS, it is essential to have a technique that can be used under both sets of conditions. For this purpose, we studied the intrinsic tyrosine fluorescence of PLB. Between 300 and 400 nm, the fluorescence emission spectrum of WT-PLB arises exclusively from its single tyrosine, Tyr-6 (Figure 3). The emission maximum of WT-PLB is 310 nm, similar to that of free tyrosine (data not shown), and characteristic of tyrosine in a homogeneous environment. For Y6W-PLB, the spectrum peaks at 350 nm and is characteristic of tryptophan in a homogeneous environment.

*Effects of PLB Phosphorylation on Its Intrinsic Fluorescence*. Figure 3 shows the effects of PLB phosphorylation on the Tyr-6 fluorescence of WT-PLB (first row) and L37A-PLB (second row), and the Trp-6 fluorescence of Y6W-PLB (third row). The measurements were carried out on samples prepared in SDS or OG solutions and in DOPC bilayers. Phosphorylation increased the fluorescence intensity in all cases, except for Y6W in SDS solution (Figure 3 and Table 1). Both WT-PLB and L37A-PLB behave similarly in the detergents SDS and OG and in DOPC bilayers, with regard to the phosphorylation response, suggesting that phosphorylation induces a structural change in both WT-PLB and L37A-PLB that increases Tyr-6 fluorescence. Since the fluorescence of *N*-acetyl-Tyr-amide increases with decreasing solvent polarity (data not shown), the increase of Tyr-6 fluorescence upon PLB phosphorylation suggests decreased polarity in the microenvironment of Tyr-6.

For Y6W-PLB, phosphorylation caused a fluorescence increase similar to that observed for WT-PLB and L37A-PLB, except in SDS solution, where there was no significant change in fluorescence (Figure 3, lower left). This anomalous response of Y6W-PLB to phosphorylation in SDS is apparently due to a special interaction between SDS and this mutant, as suggested by light scattering. Although PLB and most of its mutants (including phosphorylated Y6W-PLB) show very low light scattering in SDS solution, the unphosphorylated Y6W-PLB exhibits very high light scattering in SDS, suggesting increased micelle size or aggregation (data not shown), and making fluorescence measurement less reliable. Increasing the SDS concentration from 0.1% (Figure 3) to 0.5% greatly decreased the light scattering in solutions of Y6W-PLB and produced fluorescence results that were qualitatively similar to those observed for WT-PLB and L37A-PLB (data not shown).

*Effect of Phosphorylation on Fluorescence Quenching by Acrylamide*. Solvent accessibility of Tyr-6 and Trp-6 was studied by acrylamide quenching of fluorescence. The slope of the modified Stern−Volmer plot (Figure 4) reveals the relative accessibility of Tyr-6 and Trp-6 to the solvent. Most of the plots, especially those obtained in SDS solution for both WT-PLB and L37A-PLB, exhibit upward curvature, suggesting the presence of both dynamic and static quenching mechanisms (*30*). Nevertheless, the initial slopes indicate the relative accessibility of Tyr-6 or Trp-6 to the solvent (Table 3). For WT-PLB and L37A-PLB, the slope (accessibility) is greater in SDS than in DOPC. In both SDS and DOPC, the slope is less for WT-PLB than for L37A-PLB. Phosphorylation decreases the slope in all cases except Y6W-PLB in SDS solution, indicating decreased solvent accessibility of Tyr-6 and Trp-6. The quenching results are consistent with those of fluorescence intensity, suggesting that phosphorylation causes a structural change in PLB that decreases the solvent accessibility of Tyr-6.

*Lys-C Treatment.* In order to study the role of nearby amino acids on the phosphorylation-induced increase in Tyr-6 fluorescence, we used an endoproteinase, Lys-C, which cleaves PLB at the C-terminal end of Lys-3. Lys-C treatment of PLB increased Tyr-6 fluorescence (Figure 5), mimicking the effect of phosphorylation. This result suggests that amino acid residues at the N-terminal of PLB (1 through 3) promote a conformation that increases the exposure of Tyr-6 to the solvent, or that one or more of these residues quenches Tyr-6 fluorescence directly.

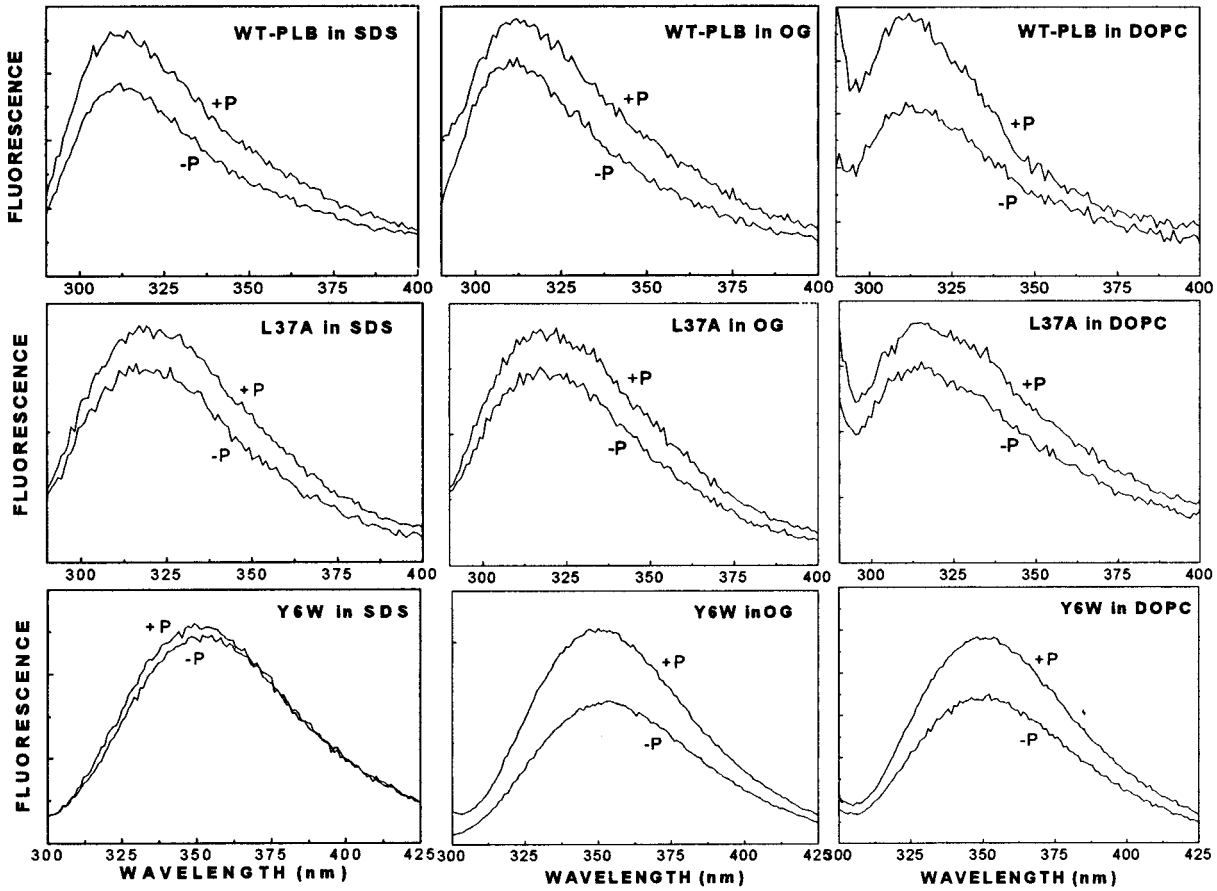


FIGURE 3: Intrinsic fluorescence emission spectra of WT-, L37A-, and Y6W-PLB in detergent (SDS and OG) solutions and lipid (DOPC) bilayers. +P, phosphorylated; −P, unphosphorylated. The excitation wavelength was 275 nm for tyrosine, and 290 nm for tryptophan.

Table 2: Effects of Phosphorylation on the Light Scattering of WT, L37A, and Y6W-PLB

| % increase upon phosphorylation | WT | L37A | Y6W |
|---|---|---|---|
| in SDS | $35 \pm 7^b$ | $0 \pm 5$ | $-75 \pm 2$ |
| in OG | $640 \pm 20$ | $0 \pm 3$ | $710 \pm 20$ |
| in DOPC | $37 \pm 5$ | $27 \pm 6$ | $52 \pm 5$ |

[a] Light scattering was measured as the peak intensity at the excitation wavelength in the emission spectra. [b] Mean ± SEM; $n = 6$ for WT-PLB, $n = 4$ for the mutants L37A and Y6W.

*CD Measurements: Effects of Phosphorylation.* To assess the effects of phosphorylation on the secondary structure of PLB, we performed CD measurements for two reasons: (a) the Lys-C experiment suggests that an increase in Tyr-6 fluorescence could be due to a change in the secondary structure of PLB; and (b) previous CD measurements on PLB have not included the L37A mutant and have not been done under buffer conditions identical to those of SDS−PAGE, and thus comparable to those of the fluorescence studies in Figure 3. The CD spectrum of WT-PLB in SDS is very similar to that of L37A-PLB (Figure 6), both indicating largely helical structures, and phosphorylation has little or no effect on the spectrum. Quantitative analysis of the CD spectra indicates no significant change in the secondary structures of WT-PLB or L37A-PLB upon phosphorylation.

## DISCUSSION

Phosphorylation decreases the mobility of PLB on SDS−PAGE (Figure 1), confirming previous reports (*11*). Ferguson plot analysis (Figure 2) suggests that this mobility shift is caused by a conformational change that increases the effective Stokes radius. CD spectroscopy showed that PLB is predominantly α-helical in the SDS−PAGE buffer and that its secondary structure does not change significantly upon PLB phosphorylation (Figure 6). However, we detected a phosphorylation-induced structural change near the N-terminus of PLB by studying the fluorescence of Tyr-6, the sole intrinsic fluorophore of PLB.

*Phosphorylation-Induced Change in WT-PLB.* Phosphorylation increased the Tyr-6 fluorescence of PLB in SDS, OG solutions, and DOPC bilayers (Figure 3), suggesting a structural change in PLB that shields Tyr-6 more from the solvent, which was confirmed by fluorescence quenching (Figure 4). Phosphorylation also increased light scattering, and this is most significant when PLB is in OG solution: Phosphorylation increased the light scattering by 640 ± 20% in OG, compared to 35 ± 7% and 37 ± 5% in SDS and DOPC (Table 2). Large aggregates can be seen when PLB is phosphorylated in OG solution. This probably occurs because phosphorylation decreases the net positive charge of PLB, decreasing the electrostatic repulsion between PLB molecules and promoting aggregation. This aggregation is much more extensive in the nonionic detergent OG than in the anionic detergent SDS, where there are counterions to shield the multiple ionic charges on PLB and facilitate solubilization. The light-scattering increase is much smaller in DOPC than in OG, suggesting that the lipid hydrocarbon chains are more effective in solvating PLB and keeping it from forming large aggregates. Phosphorylation caused a

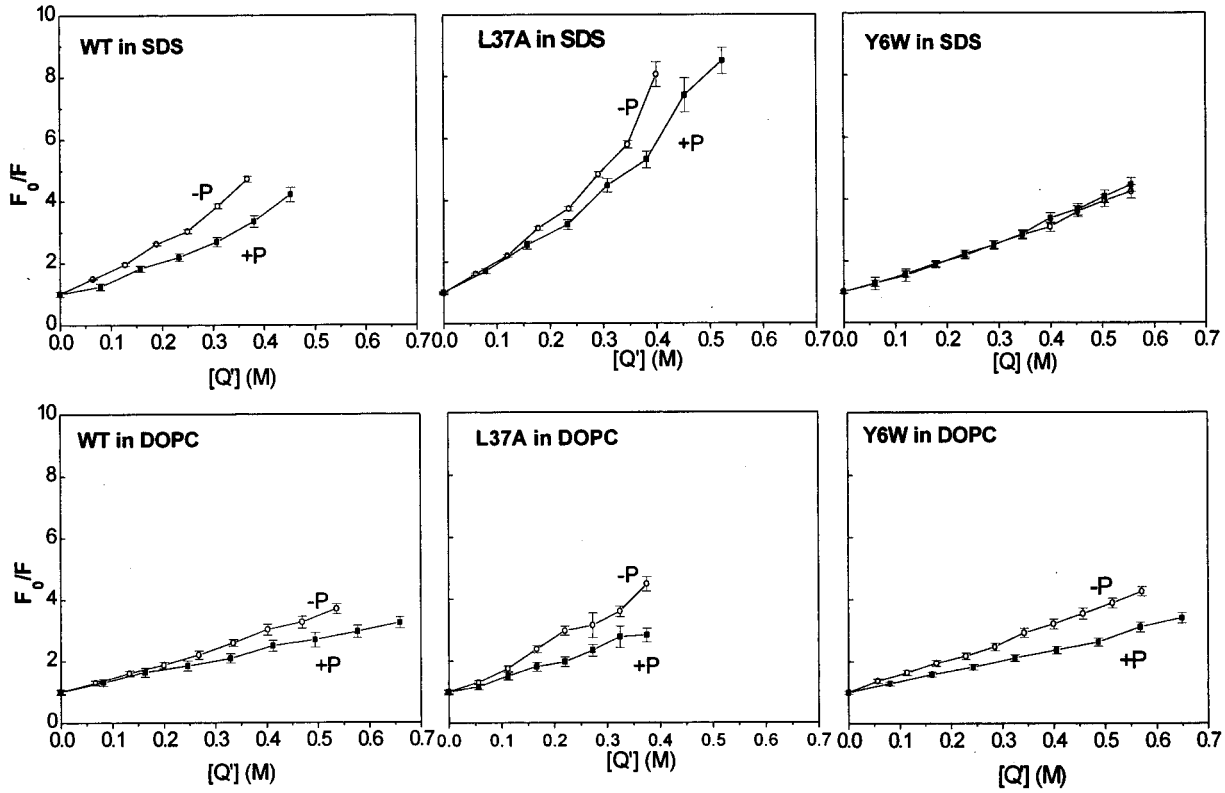


FIGURE 4: Effect of phosphorylation on acrylamide quenching of PLB fluorescence in SDS solution and lipid (DOPC) bilayers. $F_0$ and $F$ are the fluorescence intensities without and with acrylamide, respectively, and [Q′] is the effective quencher concentration, corrected for the effect of phosphorylation on quantum yield (eqs 2 and 3). (○) Unphosphorylated. (■) Phosphorylated. Each error bar shows the SEM from six measurements. The excitation and emission wavelengths were 275 and 310 nm for WT and L37A-PLB, and 290 and 350 nm for Y6W-PLB.

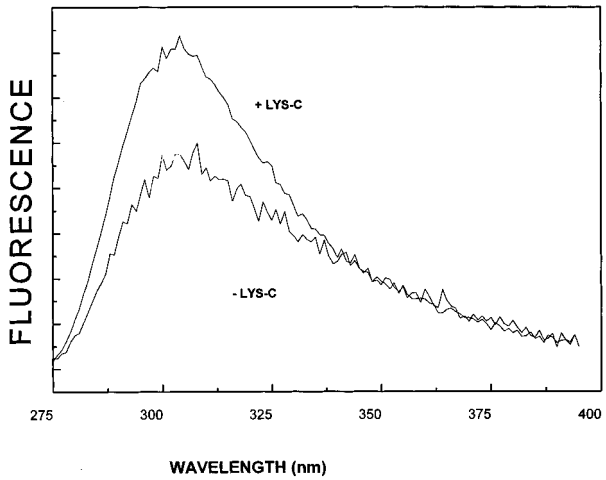


FIGURE 5: Endoproteinase Lys-C treatment on PLB Tyr-6 fluorescence in SDS solution. The excitation wavelength was 275 nm. WT-PLB was digested overnight with endoproteinase Lys-C at a ratio of PLB/Lys-C = 60 (w/w) in a buffer of 0.1 M $NaHCO_3$, pH 9, and 0.1% SDS, at 30 °C. 86% of PLB was cleaved, as measured by TNBS (2,4,6-trinitrobenzenesulfonic acid).

35 ± 7% increase in PLB light scattering in SDS, suggesting an increase either in aggregation or in the Stokes radius of the solubilized PLB. Since SDS−PAGE showed no significant change in PLB aggregation (Figure 1), we propose that *the increase in PLB light scattering corresponds to an increase in the Stokes radius of PLB upon phosphorylation*.

*Monomeric Mutant L37A.* To determine whether the detected conformational change of PLB depends on its oligomeric state, we investigated the mutant L37A-PLB, which is monomeric in SDS−PAGE (*20*, Figure 1 in the present study) and in DOPC bilayers (*22*). The electrophoretic mobility of L37A-PLB decreased upon phosphorylation, as reported previously for WT-PLB (*11*, Figure 1 in the present study). Similarly, phosphorylation induced essentially identical changes in the Tyr-6 fluorescence of L37A-PLB and WT-PLB (Figure 3), in detergent solution as well as in DOPC bilayers. These results show clearly that the phosphorylation-induced conformational change in SDS, revealed by gel shift and by tyrosine fluorescence, does not depend on the oligomeric state of PLB. In OG solution and DOPC bilayers, phosphorylation induced an increase in Tyr-6 fluorescence that is similar to that observed in SDS (Figure 3), indicating a similar protein conformational change in both WT-PLB and L37A-PLB. Since spin-label electron paramagnetic resonance in DOPC bilayers has shown that WT-PLB is primarily pentameric and L37A-PLB is primarily monomeric (*22*), these results suggest that *the phosphorylation-induced increase in tyrosine fluorescence corresponds to a conformational change within the PLB protomer and does not depend on oligomeric interactions between protomers*. These results are consistent with experiments showing that L37A-PLB is a good regulator for cardiac SR Ca-ATPase (*31*).

*Tryptophan Mutant Y6W.* The tryptophan-containing mutant Y6W-PLB permitted the study of PLB fluorescence with a higher quantum yield and better sensitivity. SDS−PAGE shows that Y6W-PLB has a similar mobility as that of WT-PLB, and phosphorylation causes the same gel shift (Figure 1). The effect of phosphorylation on Y6W-PLB

Table 3: Effect of Phosphorylation on Acrylamide Quenching of WT, L37A, and Y6W-PLB Fluorescence

| | WT | | | L37A | | | Y6W | | |
|---|---|---|---|---|---|---|---|---|---|
| initial slope | −P[a] | +P | % decrease | −P | +P | % decrease | −P | +P | % decrease |
| in SDS | 9.9 ± 1.7[b] | 6.3 ± 1.1 | 37 ± 2.8 | 12.4 ± 2.1 | 11.5 ± 1.2 | 8 ± 3.3 | 5.5 ± 0.7 | 5.8 ± 0.5 | −5 ± 1.2 |
| in DOPC | 4.9 ± 0.6 | 3.4 ± 0.2 | 31 ± 0.8 | 8.5 ± 0.9 | 5.0 ± 0.5 | 42 ± 1.4 | 5.5 ± 0.3 | 3.5 ± 0.2 | 36 ± 0.5 |

[a] −P, unphosphorylated; +P, phosphorylated. [b] Initial slopes ($M^{-1}$) from plots in Figure 3; mean ± SEM, $n = 6$.

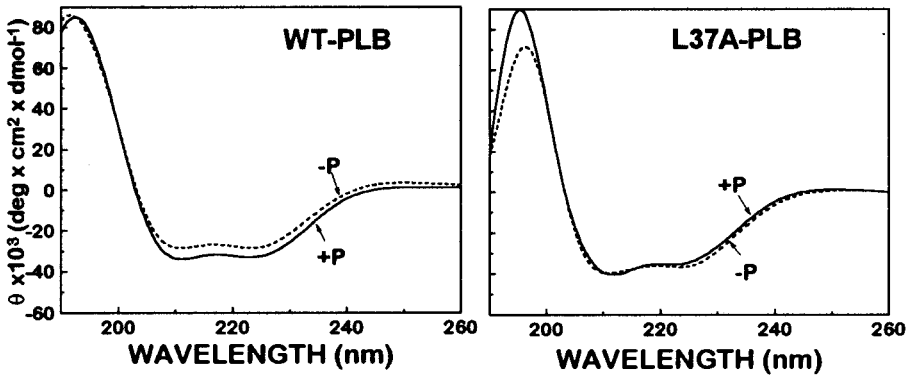


FIGURE 6: Effect of phosphorylation on the CD spectrum of WT-PLB and L37A-PLB in SDS−PAGE running buffer. The experimental conditions are described under Materials and Methods. The α-helical contents were calculated to be 88 ± 5% for the unphosphorylated WT-PLB and 90 ± 4% for the phosphorylated WT-PLB. For L37A-PLB, the α-helical contents were 79% ± 5% for the unphosphorylated and 81 ± 5% for the phosphorylated sample. For WT-PLB in OG (data not shown), the α-helical contents were 78 ± 5% (unphosphorylated) and 77 ± 5% (phosphorylated).

fluorescence (increased intensity) is similar to that of WT-PLB in OG and DOPC (Figure 3), suggesting a structural change in Y6W-PLB that shields Trp-6 more from the solvent. The fluorescence intensity increase is greater in Y6W-PLB compared to that in WT and L37A-PLB (45% vs 22%), but this difference is not easily interpreted, since the environmental sensitivities of tyrosine and tryptophan fluorescence are different. The anomalous behavior of Y6W-PLB in SDS, with regard to the effect of phosphorylation, suggests a special interaction between SDS and Y6W-PLB: Y6W-PLB appears to form larger aggregates than WT-PLB or L37A-PLB under fluorescence conditions, and this correlates with anomalous fluorescence results in SDS. Nevertheless, the results from the measurements in OG and DOPC, where light scattering by Y6W-PLB was not anomalous, showed an increase in fluorescence intensity with phosphorylation, similar to that observed for WT-PLB and L37A-PLB. Thus, although it is remarkable that the mutation of Tyr-6 to Trp has such a large effect on PLB's apparent solubility in SDS, we conclude that phosphorylation induces a similar structural change in WT, L37A, and Y6W-PLB.

*Acrylamide Quenching of PLB Fluorescence.* The initial slope of the modified Stern−Volmer plot (Figure 4) reveals the accessibility of the fluorophore to the solvent. In WT-PLB and L37A-PLB, Tyr-6 is more accessible to the solvent in SDS than in DOPC, suggesting a shielding effect from DOPC bilayers. Tyr-6 is also more accessible to solvent in L37A-PLB than in WT-PLB; this could be due to the decreased structural order of L37A-PLB, as suggested by both SDS−PAGE (Figure 1), which shows that L37A-PLB is monomeric, and CD (Figure 6), which shows that L37A-PLB is slightly less helical than WT-PLB. Phosphorylation decreases the solvent accessibility of Tyr-6 of both WT-PLB and L37A-PLB (Figure 4). The results for the quenching of Trp-6 fluorescence of Y6W-PLB are similar (Figure 4), except for the anomalous results in SDS. The fluorescence quenching results are consistent with those of fluorescence intensity, indicating that phosphorylation causes a structural change in the PLB protomer that decreases the solvent accessibility of Tyr-6.

*Lys-C-Induced Fluorescence Change in PLB.* In order to study the putative effect of secondary structural features on Tyr-6 fluorescence of PLB, an endoproteinase, Lys-C, was used. The rationale for this experiment was that tyrosine fluorescence has been previously reported to be affected by the local protein secondary structure. For example, hydrogen bonding between tyrosine and aspartate side chains in proteins usually quenches tyrosine fluorescence (*32*−*33*, *30*). Both sequence analysis (*36*) and NMR in SDS (*9*) suggested that the N-terminal part of PLB is α-helical (3.6 residues per turn), which would put Asp-2 in a favorable position to interact with Tyr-6 to form a hydrogen bond. If this is true, Lys-C treatment, which cleaves PLB at the C-terminal end of Lys-3, would eliminate this quenching hydrogen bond and thus increase Tyr-6 fluorescence. Indeed, we observed a 23 ± 8% increase in Tyr-6 fluorescence (Figure 5), providing further support to the conclusion that Tyr-6 fluorescence is reporting structural changes in the N-terminal region of PLB. Although there are many possible explanations for these results, the simplest is that the cytoplasmic part of PLB forms an α-helical structure from Asp-2 through Tyr-6, and this structure is at least partially disrupted by phosphorylation. Since CD indicates that phosphorylation does not change the α-helical content by more than a few percent (Figure 6), any change in secondary structure must be quite localized.

*Relationship to Other Work.* Previous studies of PLB phosphorylation showed that the gel mobility of PLB shifts upon phosphorylation (*11*). Our present work, using electrophoretic and spectroscopic analysis, shows that this mobility shift corresponds to a structural change in the N-terminal region of PLB that can be detected by fluorescence in the presence and absence of SDS. Electrophoretic

mobility changes of proteins upon phosphorylation were previously reported (*13*, *14*), but the mechanism of these gel shifts has not been elucidated. In the present study, we have used spectroscopic methods to study the protein structure under the conditions of electrophoresis, in order to correlate the gel mobility with protein conformation. Although the fluorescence increase correlates with the increase in Stokes radius revealed by SDS−PAGE (Figure 2), it is not necessarily true that these effects are both caused by the same structural change in PLB. For example, it is possible that the fluorescence change is due to a localized effect of the charge environment of Tyr-6. However, it seems more likely that the effects are due to steric changes that affect solvent accessibility of the fluorophore at position 6, since similar results were obtained in DOPC for Tyr and Trp at this position (Figure 3), and the results of acrylamide quenching confirm decreased solvent accessibility (Figure 4).

Other spectroscopic studies of PLB in solution have been done in various solvents (*15*, *16*, *37*, *9*). None of these was carried out under the precise conditions of SDS−PAGE (0.1% SDS), and none measured fluorescence, so a detailed comparison with the present study is not warranted. However, our CD results agree with others that there is little or no change in the secondary structure of PLB upon phosphorylation (*15*).

Two previous spectroscopic studies employing ATR-FTIR (attenuated total reflection Fourier transform infrared) spectroscopy have been carried out on PLB in lipid bilayers. Arkin et al. (*17*) reported no significant change for PLB in DMPC bilayers due to phosphorylation, but Tatulian et al. (*10*) reported significant changes, in both DMPC and POPC bilayers, which were interpreted to suggest conformational changes in the N-terminal domain, including a slight decrease in helicity due to phosphorylation. Our Tyr-6 fluorescence measurements of lipid-reconstituted PLB, revealing a significant conformational change upon phosphorylation, are consistent with the conclusions of Tatulian et al. (*10*).

Our results, showing similar changes in Tyr-6 fluorescence of WT-PLB (mainly pentameric) and L37A-PLB (monomeric) upon phosphorylation, provide structural support for the finding that L37A-PLB is fully functional in regulating the Ca-ATPase of cardiac SR (*31*, *38*). However, our observation, that the N-terminal conformational changes revealed by Tyr-6 fluorescence do not depend on whether PLB is pentameric or monomeric, does not imply that oligomeric changes play no role in PLB function. A recent EPR study showed that both WT-PLB and L37A-PLB increase their oligomeric interactions upon phosphorylation in lipid bilayers (*22*), leading to the proposal that increased aggregation of PLB is part of the mechanism by which phosphorylation decreases the inhibitory effect of PLB on the Ca-ATPase.

Ca-pump inhibition by PLB is due to a direct interaction between the two proteins, and phosphorylation relieves this inhibition by disrupting the inhibitory interaction (*39*), thus reversing the inhibitory PLB-induced aggregation of the Ca-pump molecules (*4*). Phosphorylation might accomplish this reversal simply by decreasing the positive charge on PLB, thus decreasing PLB's affinity for a negatively-charged binding site on the pump (*4*). Nevertheless, the relief of inhibition might also depend on a structural change of PLB (*10*). The results from the present study, showing a significant change in the Tyr-6 fluorescence upon phosphorylation at Ser-16 by PKA, support the structural change hypothesis.

*Conclusions.* This is the first fluorescence study of PLB, and the first study to compare directly PLB structure in SDS solution with that in lipid bilayers. Our results show that although the global change in PLB's secondary structure upon phosphorylation is rather insignificant, PLB undergoes a localized conformational change near the N-terminus that decreases the solvent accessibility of Tyr-6. This structural change occurs no matter whether PLB is in detergent solution (SDS, OG) or lipid (DOPC) bilayers, and it probably corresponds to the phosphorylation-induced gel shift of PLB in SDS−PAGE. Furthermore, the fluorescence of the monomeric mutant L37A-PLB shows that the sensitivity of this structural change to phosphorylation does not depend on interprotomer (oligomeric) interactions of PLB. This is consistent with models in which the PLB monomer is sufficient for the phosphorylation-dependent regulation of the Ca-ATPase (*22*, *31*). Thus, phosphorylation induces an intraprotomer conformational change in the N-terminal domain of PLB that can be monitored by fluorescence, using either WT-PLB or mutant Y6W-PLB, which offers greatly increased sensitivity. Future studies will be required to determine the relationship between this conformational change and the changes in Ca-ATPase self-association and activity that also accompany PLB phosphorylation (*4*).

## ACKNOWLEDGMENT

We thank Howard Kutchai, John C. Voss, James E. Mahaney, and Sampath Ramachandran for helpful discussions; and Roberta J. L. Bennett, Renhao Li, Edmund C. Howard, Nicoleta Cornea, and Christine Karim for technical assistance.

## REFERENCES

1. Lindemann, J. P., Jones, L. R., Hathaway, D. R., Henry, B. G., and Watanabe, A. M. (1983) *J. Biol. Chem. 258*, 464−471.
2. Tada, M., and Kadoma, F. (1989) *BioEssays 10*, 163−169.
3. Tada, M., and Katz, A. M. (1982) *Annu. Rev. Physiol. 44*, 401−423.
4. Voss, C. J., Jones, L. R., and Thomas, D. D. (1994) *Biophys. J. 67*, 190−196.
5. Wegener, A. D., Simmerman, H. K. B., Lindemann, J. P., and Jones, L. R. (1989) *J. Biol. Chem. 264*, 11468−11474.
6. Sham, J. S. K., Jones, L. R., and Morad, M. (1991) *Am. J. Physiol. 261*, H1344−1348.
7. Luo, W., Grupp, I. L., Harrer, J., Ponniah, S., Grupp, G., Duffy, J. J., Doetschman, T., and Kranias, E. G. (1994) *Circ. Res. 75*, 401−409.
8. Xu, Z. C., and Kirchberger, M. A. (1989) *J. Biol. Chem. 264*, 16644−16651.
9. Mortishire-Smith, R., Pitzenberger, S., Garsky, V. M., Burke, C., Mach, H., Middaugh, C. R., and Johnson, R. G. (1995) *Biochemistry 34*, 7603−7613.
10. Tatulian, S. A., Jones, L. R., Reddy, L. G., Stokes, D. L., and Tamm, L. K. (1995) *Biochemistry 34*, 4448−4456.
11. Wegener, A. D., and Jones, L. R. (1984) *J. Biol. Chem. 259*, 1834−1841.
12. Wegener, A. D., Simmerman, H. K. B., Lipnieks, J., and Jones, L. R. (1986) *J. Biol. Chem. 261*, 5154−5159.
13. Zhang, J., and Gorden, J. L. (1991) *J. Biol. Chem. 266*, 2297−2302.
14. Skalhegg, B. S., Landmark, B., Foss, K. B., Lohmann, S. M.,

Hansson, V., Lea, T., and Jahnsen, T. (1992) *J. Biol. Chem. 267*, 5374−5379.
15. Simmerman, H. K. B., Lovelace, D. E., and Jones, L. R. (1989) *Biochim. Biophys. Acta 997*, 322−329.
16. Terzi, E., Poteur, L., and Trifilieff, E. (1992) *FEBS Lett. 309*, 413−416.
17. Arkin, I. T., Rothman, M., Ludlam, C. F. C., Aimoto, S., Engelman, D. M., Rothschild, K. J., and Smith, S. O. (1995) *J. Mol. Biol. 248*, 824−834.
18. Cornea, R. L., Kobayashi, Y., Karim, C. B., Jones, L. R., and Thomas, D. D. (1995) *Biophys. J. 68*, A312.
19. Reddy, L. G., Pace, R. C., Jones, L. R., and Stokes, D. L. (1994) *Biophys. J. 66*, A201.
20. Simmerman, H. K. B., Kobayashi, Y. M., Autry, J. M., and Jones, L. R. (1996) *J. Biol. Chem. 271*, 5941−5946.
21. Schaffner, W., and Weissman, C. (1973) *Anal. Biochem. 56*, 502−514.
22. Cornea, R. L., Jones, L. R., Autry, J. M., and Thomas, D. D. (1997) *Biochemistry 36*, 2960−2967.
23. Ferguson, K. A. (1964) *Metab. Clin. Exp. 13*, 985−1002.
24. Hedrick, J. L., and Smith. A. J. (1968) *Arch. Biochem. Biophys. 126*, 155−164.
25. Porzio, M. A., and Pearson, A. M. (1977) *Biochim. Biophys. Acta 490*, 135−167.
26. Jones, L. R., Simmernan, J. K. B., Wilson, W. W., Gurd, F. R. N., and Wegener, A. D. (1985) *J. Biol. Chem. 260*, 7721−7730.
27. Sreerama, N., and Woody, R. W. (1993) *Anal. Biochem. 209*, 32−44.
28. Li, C., Wang, J., and Colyer, J. (1990) *Biochemistry 29*, 4535−4540.
29. Watanabe, Y., Kijima, Y., Kadoma, M., Tada, M., and Takagi, T. (1991) *J. Biochem. 110*, 40−45.
30. Lakowicz, J. R. (1986) in *Principles of Fluorescence Spectroscopy*, pp 359−364, Plenum Press, New York.
31. Autry, J. M., and Jones, L. R. (1997) *J. Biol. Chem. 272*, 15872−15880.
32. Riehm, J. P., Broomfield, C. A., and Scheraga, H. A. (1965) *Biochemistry 4*, 760−771.
33. Hoppe, W., Lohmann, W., Markl, H., and Ziegler, H. (1986) in *Biophysics*, pp 250−251, Springer-Verlag Inc., New York.
34. Szabo, A. G., and Rayner, D. M. (1978) *J. Am. Chem. Soc. 102*, 554−563.
35. Lee, K. J., Ross, R. T., Thampi, S., and Leugans, S. (1992) *J. Phys. Chem. 96*, 9158−9162.
36. Fujii, J., Ueno, A., Kitano, K., Tanaka, S., Kadoma, M., and Tada, M. (1987) *J. Clin. Invest. 79*, 301−304.
37. Hubbard, J. A., Maclachlan, L. K., Meenan, E., Salter, C. J., Reid, D. G., Lahouratate, P., Humphries, J., Steven, N., Bell, D., Neville, W. A., Murray, K. J., and Darker, J. G. (1994) *Mol. Membr. Biol. 11*, 263−269.
38. Kimura, Y., Kurzydlowski, K., Tada, M., and MacLennan, D. H. (1996) *J. Biol. Chem. 271*, 21726−21731.
39. James, P., Inui, M., Tada, M., Chiesi, M., and Carafoli, E. (1989) *Nature 342*, 902−904.

BI9801053